

Synthesis of ceramic membranes

Part I *Synthesis of non-supported and supported γ -alumina membranes without defects*

R. J. R. UHLHORN, M. H. B. J. HUIS IN'T VELD, K. KEIZER*,
A. J. BURGGRAAF

Laboratory of Inorganic Chemistry, Material Science and Catalysis, Faculty of Chemical Engineering, University of Twente, P.O. Box 217, 7500 AE, Enschede, The Netherlands

Non-supported γ -alumina films are prepared from a boehmite colloidal suspension. After calcination at 600 °C, the microstructure is characterized by a mean pore diameter of 3 nm, a porosity of 50% and a tortuosity of 5.5. The structure is formed by card packed, plate-shaped particles, giving rise to slit-shaped pores. Supported γ -alumina films, made by a slipcasting process using the same boehmite precursor, have a similar structure as the non-supported films. The slipcasting process is very sensitive to support characteristics and frequently yields defect films. Polyvinylalcohol (PVA) (molecular weight 72000 g mol⁻¹) is added to the boehmite precursor (0.25 g g⁻¹ film) to improve this process. This addition results in a less critical and better controllable drying and calcining procedure. The addition of PVA is necessary to slipcast defect free γ -alumina films on supports with pore diameters of 0.4 μ m or smaller and on multi-layer supports. It has no significant effect on the resultant microstructure of the γ -alumina film, provided all PVA is removed by appropriate thermal treatment. The slipcasting rate is slower, resulting in thinner films of 3-5 μ m at identical slipcasting times.

1. Introduction

The preparation of inorganic membranes has received much attention in the past few years [1]. Especially glass membranes [2] and ceramic oxide membranes [3] have been of interest. Commercial applications of alumina membranes can nowadays be found in the wine and beer clarification and the pharmaceutical industry.

An oxide membrane, employed in separation processes with a pressure gradient, consists of a thin separation layer and a porous carrier, which serves as a support. The most frequently used configuration in our laboratory is depicted in Fig. 1. In commercial applications, the support itself also consists of two or more layers (Fig. 2). The support has pores typically of 10-15 μ m diameter and a porosity around 40%. The pore diameter diminishes with each successive layer, typically to 0.2-1 μ m in the second layer and 3-100 nm in the third. Details of the preparation of such system are not given by industrial organizations.

More is known of the preparation of the thin ultrafiltration top layer [4-6]. Since this layer contains small pores (diameter < 10 nm), colloidal suspensions are used as a starting material. If the support is saturated before introducing the colloidal suspension, film-coating is the forming mechanism. The suspension is transported along the membrane surface. The viscosity and the concentration of the suspension

determines among other things the layer thickness. The disadvantage of this method is, that there is no direct interaction between the support and the deposited layer. Hence the adherence of the ultrafiltration top layer is not very good. If a dry support is brought into contact with a sol however, capillary forces are present inside the support pores. Water of the sol is sucked into the support. A layer is formed by concentration of the sol particles at the boundary of support and sol. This forming mechanism is called slipcasting. The advantage is the better adherence of the top layer. The disadvantage is, that the support must have a certain minimum pore size in order to obtain a sufficiently large capillary force and that the wetting behaviour with the sol is critical.

This slipcasting mechanism has been developed and extensively studied in our laboratory [7]. γ -Alumina membranes of 1-10 μ m thickness, having a pore diameter of 3 nm, a sharp pore size distribution and a porosity of about 50%, could be produced. They contained almost no defects in liquid separations, as demonstrated by a sharp cut-off value for polyethylene glycol (PEG) [8]. Application of these membranes for gas separation however introduced the need for absolutely pinhole free top layers because gas transport is much more sensitive to defects than liquid transport. Therefore the synthesis of the γ -alumina as described by Leenaars [7-10] had to be optimized.

* Author to whom all correspondence should be addressed.

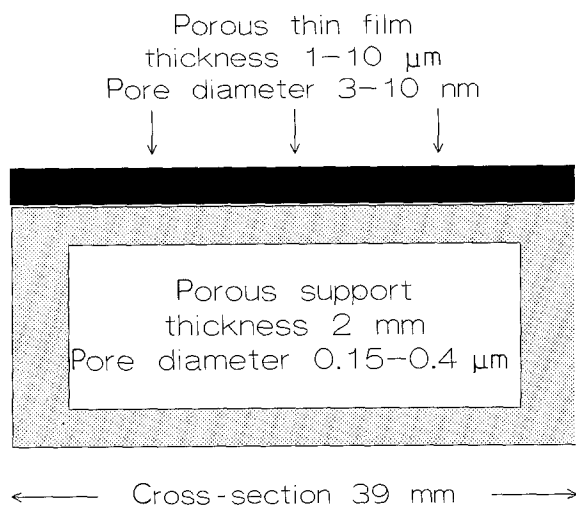


Figure 1 Schematic representation of an asymmetric composite membrane.

This article will deal with these improvements. Since this is a continuation of the work of Leenaars, a short summary of his work is given below.

It is fairly difficult to characterize the microstructure of thin, supported γ -alumina membranes. Therefore, non-supported thin films were prepared in a comparable way and characterized [9]. It was proven by N_2 adsorption-desorption measurements, that the microstructural characteristics of thin non-supported

films are similar to supported thin films [7]. The microstructure of γ -alumina membranes was therefore studied, using non-supported films.

Fig. 3 gives schematically the preparation of non-supported layers, as performed by Leenaars [9]. First a boehmite colloidal suspension (sol) was prepared. Transmission electron microscopy (TEM) measurements showed that this colloidal suspension consisted of plate-shaped particles of about 2.5-3 nm thick and at least about 30 nm in cross-section. The boehmite particles are slightly agglomerated in solution, but break up during drying. Upon drying, capillary forces are developed (Fig. 4a). These result in large compressive forces in the gel causing ordering of the structure. Plates A and B in Fig. 4a will be closer to each other than plates B and C due to the faster drying rate close to the surface. This implies that the small pores at the top (distance between plates A and B) become smaller and the large pores in the bulk (distance between plates B and C) become larger. This process would eventually lead to cracks. It is stopped however by the repulsion forces, arising from the charged particles. Finally a homogeneous, card pack structure is obtained (Fig. 4b).

The pore structure of the non-supported γ -alumina membranes was studied by N_2 adsorption-desorption measurements. Table I gives the structure as a function of calcination temperature, using a slit-shaped

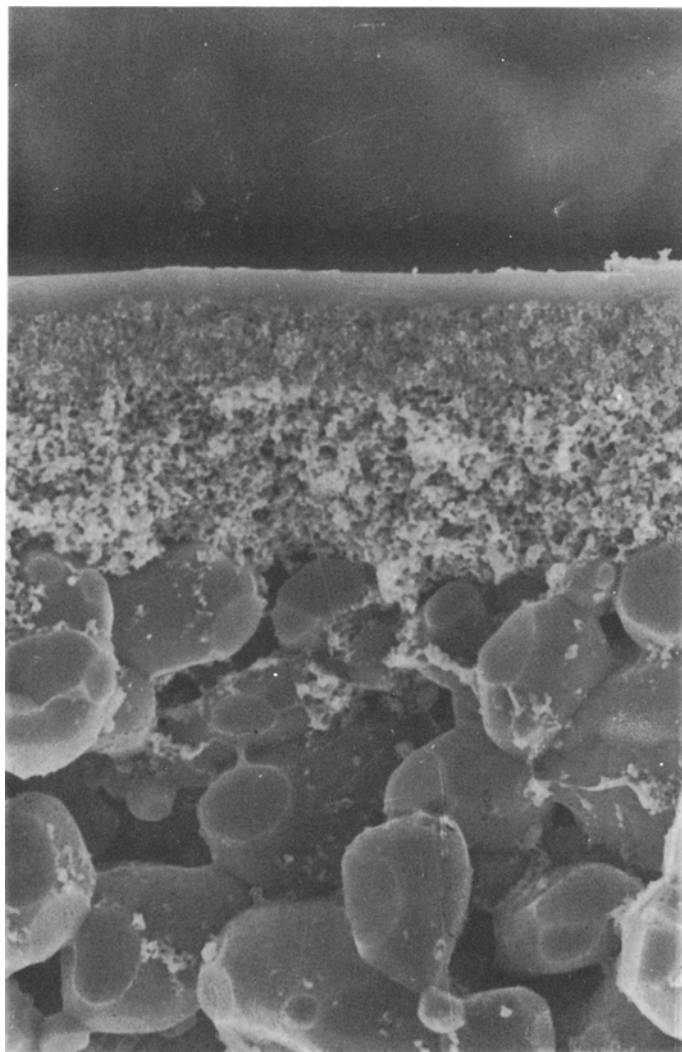


Figure 2 SEM picture of a multi-layer γ -alumina membrane. Clearly visible are the support, the first and second (micro- and ultrafiltration) intermediate layers and the colloidal (ultrafiltration) layer.

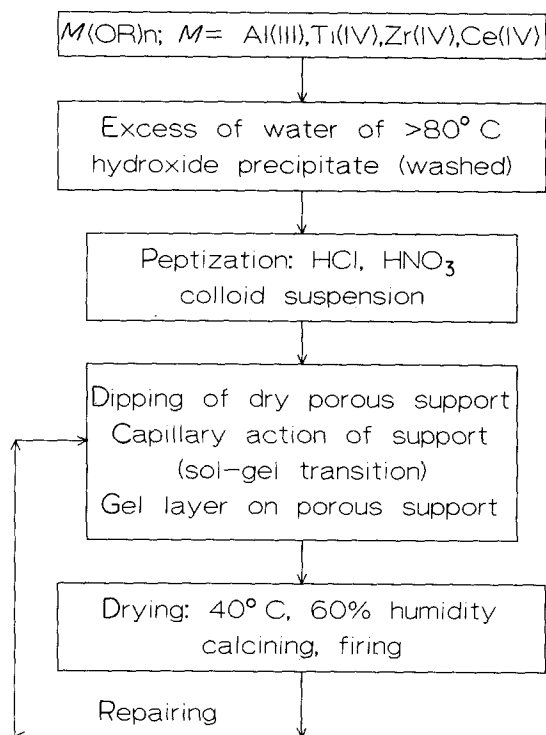


Figure 3 Schematic representation of the preparation of non-supported and supported γ -alumina thin films.

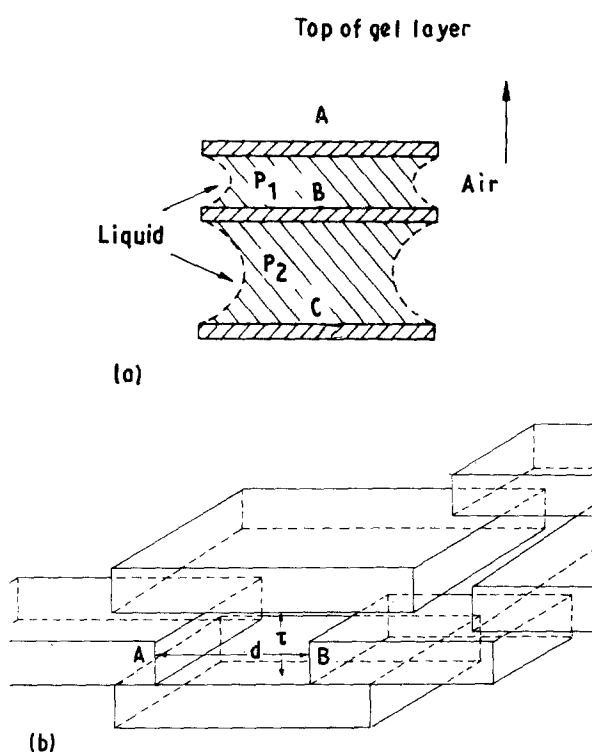


Figure 4 (a) Part of a cross-section of the gel layer when the drying process is in progress; (b) idealized model of the boehmite membrane microstructure.

pore model. It can be seen, that the pore size can be tailor made between 2.5 and 10 nm. Above 1000°C a phase transition to α -alumina occurs, destroying the microstructure (Table I). Detailed studies have been performed by Lin *et al.* [11].

Fig. 3 incorporates the preparation of supported thin films [7]. The same starting material is used. The supported membranes are made by a so-

called dipping procedure. The dry, homogeneous support is brought into contact with the boehmite sol. Due to the capillary forces, water is sucked into the pores of the support. The concentration of boehmite at the entrance of the pores increases and gelation of the sol occurs. After a certain period (in the order of seconds), the support is taken out and the gel layer is dried and calcined. The boehmite plates have a strongly preferred orientation parallel to the support, as shown by X-ray diffraction (XRD). Upon calcining, γ -alumina is formed due to dewatering of the boehmite. This phase transition is accompanied by shrinkage in lateral direction only. The strongly preferred orientation is maintained after calcination. Stresses can be relaxed by gliding of the plate surfaces. From this picture it is clear, that the drying and calcination step should be carried out very carefully, in order to prevent cracking of the system [12].

It is proven, that structural developments occur along the same lines as with non-supported films. Nitrogen adsorption-desorption experiments, performed on a large number of supported thin films, yielded a modal pore size of the supported γ -alumina film exactly equal to the modal pore size of non-supported γ -alumina films. In another experiment very thick supported γ -alumina films were made. These peeled off of the support and their structure could be determined by N_2 adsorption-desorption. They differed by less than 1% in microstructural characteristics from the non-supported γ -alumina films.

The formation of the supported layers can be described by a slipcasting mechanism. Characteristic for this mechanism is, that the layer thickness increases linearly with the square root of time. This was shown to be true for the formation of γ -alumina supported thin films [7]. Critical parameters in the slipcasting process are the pore diameter of the support, the sol concentration, the agglomeration state of the sol, the contact time and the acid used for peptization. Typically a 0.72 M boehmite sol, peptized with 0.07 M HNO_3 per mole aluminium, was brought into contact with a plate-shaped support (cross-section 39 mm, thickness 2 mm) containing pores of 0.12 μm diameter for 3 s. The resulting layer was about 4 μm thick.

Water permeability experiments showed, that the value of the tortuosity k_t (see Equation 1) of the γ -alumina supported thin films was around 5, which is 2.5 times higher than normally found. This can be understood, considering the highly tortuose, card packed structure shown in Fig. 4b. Cut-off value determination for polyethylene glycol solutions showed a sharp cut-off at a molecular weight of 2000 for a supported thin film calcined at 400°C [8]. This corresponds reasonably well to a pore diameter of 2.5 nm.

From this short review of earlier work it follows, that especially the drying and calcination steps are critical to the quality of the γ -alumina supported thin films. This results in poorly reproducible layer quality, unless very slow drying and calcining rates are used. A second problem was that although the supported γ -alumina thin films appeared pinhole free in liquid applications, they did not do so in gas transport

TABLE I Microstructural characteristics of aluminium derived thin films as a function of temperature treatment; data from Leenaars [9]

Temperature (°C)	Time (h)	Phase	BET surface (m ² g ⁻¹)	Pore size (nm)	Porosity (%)
200	34	γ-AlOOH	315	2.5 ^a	41
400	34	γ-Al ₂ O ₃	301	2.7	53
	170	γ-Al ₂ O ₃	276	2.9	53
	850	γ-Al ₂ O ₃	249	3.1	53
500	34	γ-Al ₂ O ₃	240	3.2	54
600	34	γ-Al ₂ O ₃	209	3.5	55
800	34	γ-Al ₂ O ₃	154	4.8	55
900	34	θ-Al ₂ O ₃	99	5.4	48
1000	34	α-Al ₂ O ₃	15	78 ^b	41

^a = slit-shaped pore model; ^b = cylinder shape pore model.

characterizations, as will be shown. Finally it proved to be difficult to make thin γ-alumina films on various types of supports, differing in pore diameter (distribution), surface roughness and wetting behaviour.

Therefore three improvements were introduced. First a certain amount of polyvinyl alcohol (PVA) was added to the boehmite colloidal suspension. This decreased the drying and calcination time considerably, while the layer quality became reproducible. Also the influence of the support became less critical. Second the drying step was better controlled by drying in a climate chamber at set conditions. Finally a repairing technique was introduced to further improve the quality of the top layer. It consisted of a so-called multiple dipping technique, where the formation and processing steps to prepare supported thin films were repeated.

This article describes the effect of the improvements on the microstructure and forming mechanism of the non-supported and supported thin γ-alumina films. First the influence of PVA on the microstructure of non-supported γ-alumina films will be discussed. This is followed by a discussion of the influence of PVA on the forming mechanism of γ-alumina supported thin films. The repairing technique, designed to obtain membranes without pinholes, will be discussed briefly. Finally the characterization of supported γ-alumina films by gas and liquid permeability and cut-off value determination will receive attention. It will be proven, that the microstructure of non-supported and supported alumina thin films, prepared by addition of PVA to the boehmite suspension, are essentially the same.

2. Theory: gas and liquid permeability

Liquid permeability is commonly described by the Kozeny-Carman equation [10]

$$\frac{\Delta V}{\Delta t} \frac{1}{A} = \frac{\epsilon^3}{k_0 k_t L \eta S_v^2 (1 - \epsilon)^2} \Delta P \quad (1)$$

where the left hand side represents the flux per unit area (m³ m⁻² s⁻¹), ε is the porosity, k₀ a shape factor, k_t the tortuosity (defined by the square of the ratio of the actual length travelled L_e and the thickness of the layer L; thus k_t = (L_e/L)²), L the membrane thickness, η the liquid viscosity (Ns m⁻²), S_v the internal surface area per unit volume solid material (m² m⁻³) and ΔP

the applied pressure difference. This equation is in fact the Poiseuille equation for viscous flow, adapted for a porous medium. If the volume flux per unit area is plotted as a function of the pressure drop across the membrane, a linear relation should be found. Provided the porosity and the internal surface area are known, a tortuosity can be calculated from Equation 1. This procedure was followed by Leenaars, resulting in a k_t value of 5 [10]. It will also be applied on γ-alumina thin films, made with PVA, later in this article.

In order to determine the quality of the supported top layer, a method to determine and describe gas transport through a γ-alumina supported thin film was developed [13]. Basically the gas phase permeability is represented by

$$F_0 = \frac{F}{A \Delta P} = C_1 + C_2 P_m \quad (2)$$

where F₀ is the permeability (mol m⁻² s⁻¹ Pa⁻¹), F the flow (mol s⁻¹), A the outer surface area (m²), ΔP the pressure difference, C₁ a constant representing Knudsen diffusion, C₂ a constant representing laminar flow and P_m the mean pressure in the medium. If only Knudsen diffusion occurs as transport mechanism, the permeability is no function of the mean pressure. This is the case for a γ-alumina thin film without pinholes. If both Knudsen diffusion and laminar flow are present, the permeability will be dependent on the mean pressure. This is the case for a γ-alumina thin film with pinholes. Thus the permeability as a function of the mean pressure of a supported γ-alumina thin film characterizes the quality of this thin film.

3. Experimental procedure

Boehmite (γ-AlOOH) sols were prepared by adding dropwise aluminium secondary butoxide to water, which was heated above 80 °C and stirred at high speed. About 1.5 l of water were used per mole alkoxide. After addition of the alkoxide, 0.07 mole HNO₃ per mole butoxide was added. The resulting colloidal suspension was kept boiling until most of the butanol had evaporated and was then refluxed for 16 h to form a 1 M stable boehmite sol. PVA (Merck, molecular weight 72000, residue < 0.05 wt %) solutions were made by adding 3.5 g of PVA to 100 ml of boiling

water under vigorous stirring. After addition of 5 ml 1 M HNO_3 the solution was refluxed for about 4 h. A dipping solution was prepared by pouring 20 ml of PVA solution to 30 ml of 1 M boehmite sol. Non-supported layers were prepared by drying this solution overnight in a polypropylene petri dish at 40 °C and 60% relative humidity (r.h.). The resulting gels were calcined at a rate of 60 °C h^{-1} and kept at 600 °C for 3 h. The supported γ -alumina films were prepared by dipping the support for 4 s in the dipping solution, drying for 3 h at 40 °C and 60% r.h. and calcining at a rate of 60 °C h^{-1} to 600 °C, where they were kept for 3 h.

Nitrogen adsorption-desorption experiments were performed with non-supported thin films, using a Micromeritics ASAP 2400 instrument. The liquid permeability and cut-off value determination were carried out, using a dead end vessel configuration (Fig. 5). For liquid permeability experiments, a saturated support was placed at position 8 and the vessel was filled with liquid and pressurized with nitrogen. The permeate was collected and its volume determined by weight. Accurate measurement of temperature during the measurement was possible by a PT100 element (Fig. 5, position 15). For cut-off value experiments polyethylene glycols with a molecular weight of 400, 1000, 3000, 6000 and 20000 were used (Merck). The dead end vessel of Fig. 5 was filled with a 1000 p.p.m. glycol solution, starting with the lowest molecular weight. When the total amount of permeate was 5 times the dead volume of the system, the permeate was collected. In order to prevent fouling, small pressure drops

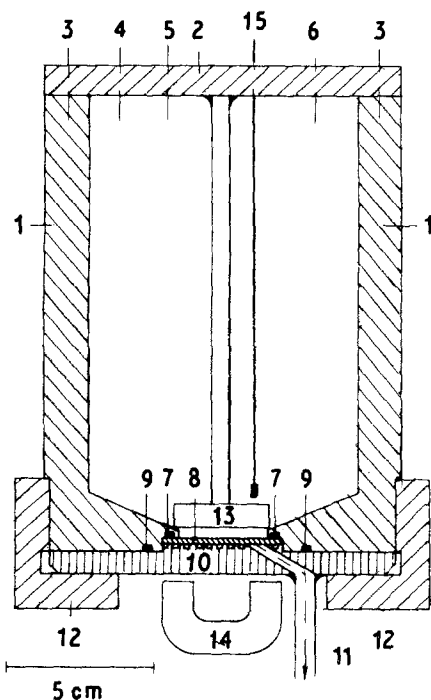


Figure 5 Permeation vessel used for the liquid filtration experiments: position 1: housing; position 2: top plate; position 3: screws; position 4: safety-valve; position 5: connection with N_2 cylinder; position 6: pressure gauge; positions 7 and 9: O-rings; position 8: support or membrane; position 10: bottom plate; position 11: outlet; position 12: part screwed on housing; position 13: magnetic stirrer; position 14: rotating magnet; position 15: PT-100 temperature measuring element.

(typically 3×10^5 Pa) were used. The glycol solution was poured out and the vessel was filled with a new glycol solution with a higher molecular weight. This procedure was repeated for all glycol solutions. The feed and permeate of each solution were analysed, using a Beckman 915 A total organic carbon analyser.

Finally, layer thicknesses of supported thin films of alumina were determined on a fractured surface, using a Jeol-JSM35CF scanning electron microscope.

4. Results and discussion

4.1. Non-supported thin films

A comparison will be made between the microstructure of γ -alumina films, made with and without PVA. For simplicity reasons, the films made with PVA are denoted as $\gamma\text{-Al}_2\text{O}_3\text{-P}$, those made without PVA by $\gamma\text{-Al}_2\text{O}_3$. All films were calcined at 600 °C during 3 h prior to the measurements. Fig. 6 presents a typical N_2 adsorption-desorption isotherm for thin $\gamma\text{-Al}_2\text{O}_3$ and $\gamma\text{-Al}_2\text{O}_3\text{-P}$ films. The isotherms are almost equal in shape, only the desorption branch from the $\gamma\text{-Al}_2\text{O}_3\text{-P}$ film is slightly more curved than the desorption branch of the $\gamma\text{-Al}_2\text{O}_3$ film. Both isotherms can be classified as a type IV isotherm with a type E hysteresis loop [14]. The type IV isotherm is the normal form of an isotherm, found with porous substances with a pore diameter larger than 2 nm. The type E hysteresis loop is normally identified with ink bottle type pores. It is now recognized however that the role of the pore network can be very important, especially in non-spherical geometries [14]. Therefore it is very difficult to assign a certain pore shape to the type of hysteresis loop.

A pore size distribution can be calculated from the desorption isotherm, applying the Kelvin equation

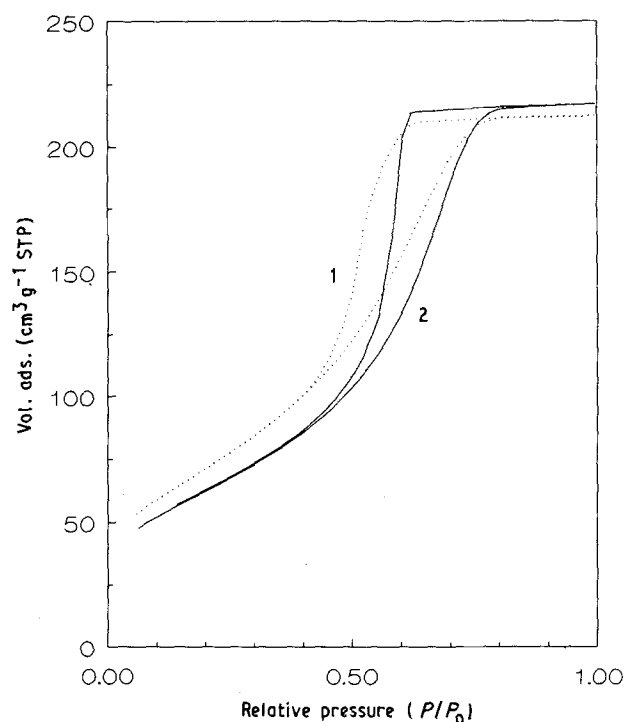


Figure 6 Adsorption-desorption isotherms of non-supported thin films, made with and without addition of PVA: (···) with PVA; (—) = without PVA.

TABLE II Comparison between structural data of non-supported thin films, made with and without PVA, from three separate boehmite suspensions (identically prepared); calcination temperature is 600 °C

PVA addition	Pore diameter (nm)		Porosity (%)	BET surface (m ² g ⁻¹)	Remarks
	slit	cylinder			
No	3.3	3.7	54	231	Sol 1
Yes	2.8	3.3	51	229	Sol 1
No	3.4	4.0	57	245	Sol 2
Yes	2.9	3.6	56	260	Sol 2
No	3.4	4.2	56	227	Sol 3
Yes	3.0	3.7	52	219	Sol 3
No	3.5	5.5	55	209	Leenaars

and assuming slit-shaped pores. This slit-shaped form is assumed, because packing of plate-shaped particles will most likely result in slit shape pores (Fig. 4b). In literature there is ample discussion on which isotherm, the adsorption or desorption isotherm, should be used for calculation of the pore size distribution [4, 14]. In the case of slit-shaped pores the choice is not difficult however, since during the adsorption no equilibrium exists. In this case the pore can be viewed as two infinite plates, slowly filling with adsorbate. Therefore only the desorption isotherm can be used. If the desorption isotherms of the γ -Al₂O₃-P and γ -Al₂O₃ thin films are compared, three important features arise:

1. The relative pressure where desorption starts, is almost equal; this indicates the same upper limit for the pore diameter.
2. The desorption isotherm for the γ -Al₂O₃-P film declines less steeply, indicating a broader distribution.
3. The relative pressure where the hysteresis loop closes again is lower for the γ -Al₂O₃-P film, indicating the presence of smaller pores.

From these points it can be concluded, that the pore size distribution of the γ -Al₂O₃-P film is broader in the small diameter range of the pore size distribution. This qualitative picture is justified by Fig. 7. In this figure the pore size distributions are presented. They were calculated assuming a slit-shaped pore and applying a *t*-layer correction [14, 15]. It can be seen, that both pore size distribution have no pores with diameters above 4 nm. The maximum for the pore diameter distribution of thin films made without PVA is slightly shifted to higher pore diameters compared with the maximum for a thin film with PVA. The effects are not very large however. Table II finally compares several structural characteristics of thin γ -Al₂O₃-P and γ -Al₂O₃ films. For comparison reasons the data of Leenaars [9] are also included. The Brunauer-Emmett-Teller (BET) surfaces in Table II were calculated from the first part of the isotherm, applying the well-known BET equation and taking 0.162 nm² as the area occupied by an adsorbed N₂ molecule [15]. Assuming that all pores are filled with liquid nitrogen at a relative pressure of 0.95, the porosity of the samples in Table II could be calculated, employing the ideal gas law [9]. The density of liquid nitrogen at 77 K was taken to be 0.808 g cm⁻³, the density of γ -alumina 3.7 g cm⁻³. From Table II and Figs 6 and 7 it can be concluded, that introduc-

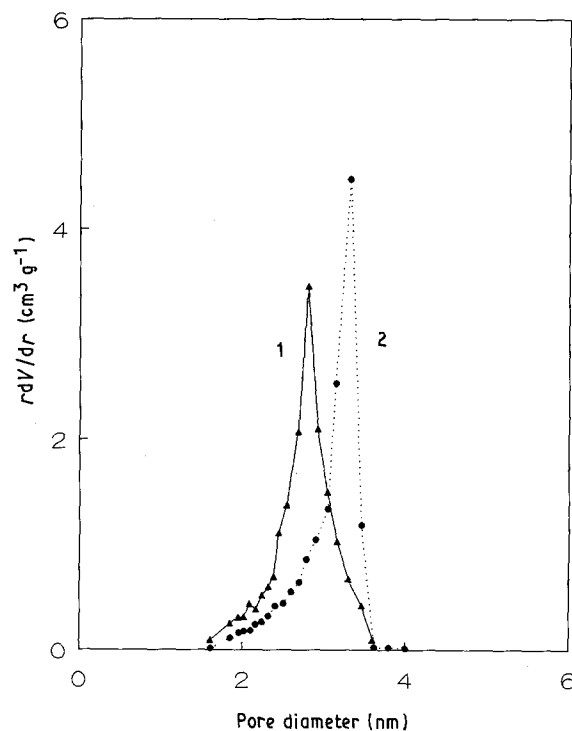


Figure 7 Pore size distributions from the desorption isotherms presented in Fig. 6: (—) = with PVA; (···) = without PVA.

tion of PVA results in only slight changes in the microstructure. The distribution curves have become slightly more symmetric with a slightly smaller mean pore diameter. This suggests a somewhat improved ordering of the particle packing.

The conclusion that introduction of PVA results in only slight changes in microstructure is slightly surprising, considering the radius of gyration of a PVA molecule with a molecular weight of 72000. This radius was calculated with the Flory-Fox equation [16] and is about 3 nm. The molecule is then larger than the thickness of the plates and hence larger than the resultant pore size. A strong effect on the pore structure is expected, but not found. Two things should be considered though. These are the shape of the PVA molecule and the pore geometry. PVA is to a large extent a linear molecule [17] and thus a radius of gyration is only a very rough estimation of the size of the molecule. The pores in the γ -alumina matrix are slit-shaped, meaning that the length of the pores is much larger than the slit-width. It is therefore very possible, that the PVA molecule is more or less stretched over the length of the slit-shaped pore. This

would only give slight distortions in the structure. It can be expected, that if large, spherical molecules are incorporated, or that if the pore geometry is different, the structure is disrupted. This would lead to a broader pore size distribution. These conclusions were experimentally verified for titania membranes with spherical particles [18].

4.2. Supported thin films

4.2.1. Forming mechanism and repairing technique

In the previous section it was concluded that addition of PVA to the colloidal boehmite suspension has some (minor) structural effects in thin non-supported films. The structure of supported and non-supported thin films is equal (see also next section). Still there can be a pronounced effect of PVA on the forming mechanism of supported thin films. For boehmite sols the forming mechanism of supported thin films could be described by slipcasting [7]. This mechanism is characterized by a linear increase of the layer thickness, L , as a function of the square root of dipping time, t , according to [7]

$$L = \frac{2\gamma \cos \beta}{\eta} C(t)^{1/2} + L_a \quad (3)$$

where γ is the surface tension (Nm^{-1}), β the contact angle between the liquid and the solid surface, C is a constant, η is the viscosity of the solution and L_a is the adhering layer thickness. When PVA is added to the dipping solution, the effective particle size and the viscosity of the solution are expected to change.

Fig. 8 illustrates the changes in the slipcasting kinetics. From this figure it is clear that in all cases slipcasting occurs, because the layer thickness in-

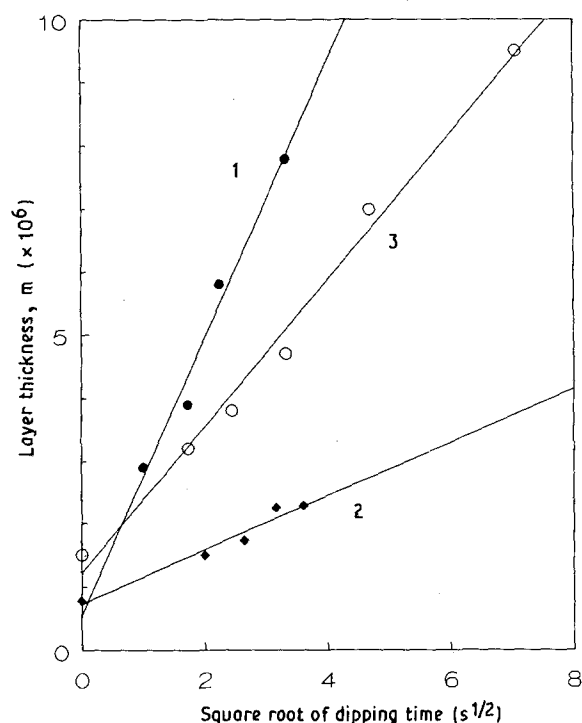


Figure 8 Increase in layer thickness per dipping procedure as a function of the square root of dipping time for a dipping solution with and without PVA: (○) = without PVA; (◆) = with PVA; (○) = second dipping procedure, without PVA.

creases linearly with the square root of dipping time (Equation 3). This increase is however much smaller if PVA is incorporated. Curve 3 is the increase in layer thickness when a second dipping procedure is applied and will be discussed later. The point at $t = 0$ s presents the minimum obtainable layer thickness, the adherent layer L_a (Equation 3). It was in all cases determined by dipping a dense α -alumina support in the dipping solution.

The lower slipcasting rate obtained with dipping solutions containing PVA can be explained by the combined effect of PVA on the viscosity and the surface tension of the dipping solution. The viscosity of the dipping solution increases by addition of PVA, leading to a lower slipcasting rate (Equation 3). This would however also lead to a thicker adherent layer. Since this is experimentally not found, another more important effect must exist. It is known, that addition of PVA to water lowers the surface tension of the solution [17]. This in turn leads to a decrease of the capillary force (which is proportional to the surface tension), and consequently the slipcasting rate is also lower (Equation 3).

After deposition of the thin film on the support, drying and calcining, the resulting thin γ -alumina films were tested for the presence of pinholes and defects by gas permeability experiments. Fig. 9a presents the permeability for helium as a function of mean pressure for the support, the support and top layer and for the top layer only. The permeability of the top layer is calculated from the experimental permeabilities of the other two. It can be seen, that the top layer permeability increases linearly with the mean pressure. This is an indication for the presence of viscous flow in the top layer and thus for pinholes. Therefore it must be concluded, that after dipping the support once, pinholes still exist in the formed top layer.

In order to remove the defects, the dipping procedure was repeated. This means, that after dipping, drying and calcining the γ -alumina supported thin film once, the whole procedure was repeated. The helium permeability of the top layer was determined and if pinholes were still present, the system was dipped again, dried and calcined. Fig. 9b gives the helium permeability as a function of mean pressure and the number of dipping procedures applied. It is clear from this figure, that after three subsequent dipping procedures, the top layer contains no pinholes anymore. The gas transport takes place by the Knudsen diffusion mechanism only.

The fact that the defects are removed by subsequent dipping procedures, can be understood as follows. At the places, where pinholes and defects are present, the support is hardly or not at all covered with a γ -alumina film. Consequently the resistance against liquid transport is much lower at the site of a pinhole than at the site of a γ -alumina film. During the next dipping procedure, water is sucked faster into the support at the pinhole site, due to this lower resistance. This again implies, that the gel layer growth is faster at the pinhole sites than at the site of the γ -alumina film. Thus the pinholes and defects are self-repairing.

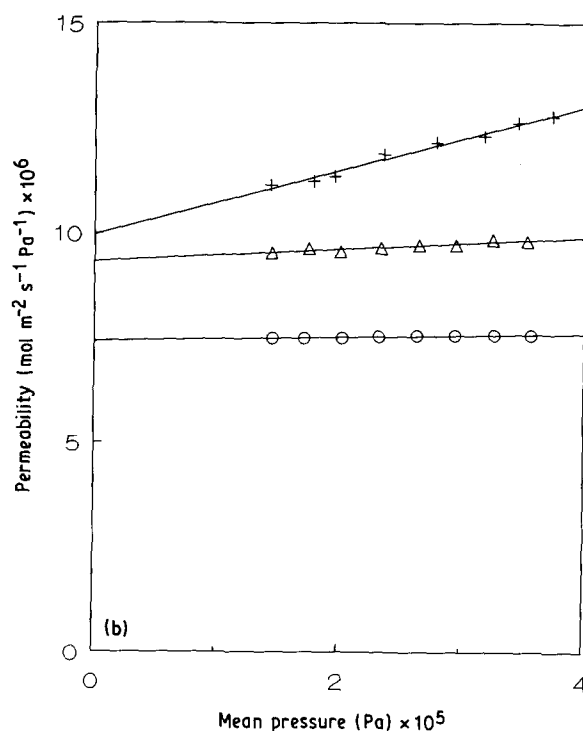
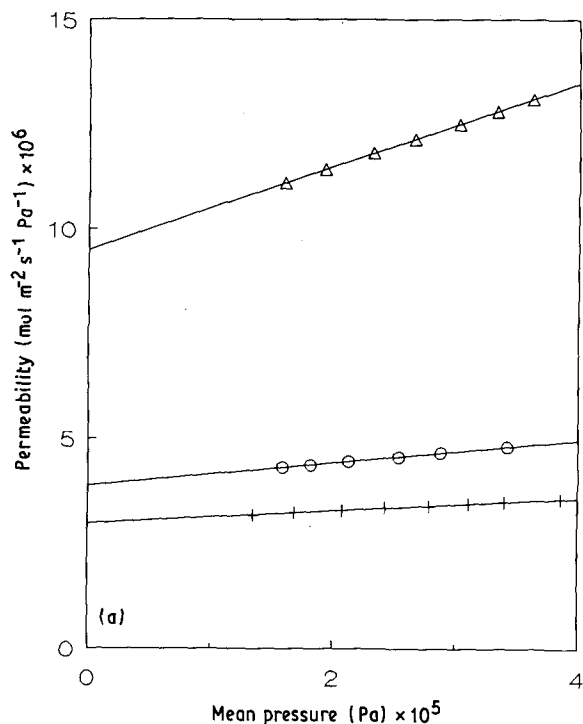


Figure 9 (a) He permeability as a function of mean pressure for a (○) support, (+) support and top layer and for (Δ) top layer only (calculated); top layer thickness is 4 μm; (b) He permeability as a function of mean pressure and of the dipping procedures applied; final top layer thickness is 8.5 μm; dipped (+) once; (Δ) twice and (○) three times.

The disadvantage of this repairing method is that the over-all layer thickness increases with subsequent dipping procedures. Fig. 8 demonstrates this. Line 3 of this figure presents the increase in layer thickness as a function of dipping time during the second dipping procedure. The total layer thickness is given by the sum of the layer thicknesses of the first and second procedure. Although the forming mechanism is still slipcasting, the layer growth is slower than during the first dipping procedure. This is due to the increased

resistance to water transport. Still, if the dipping time is only 3 s, the layer thickness almost doubles (net increase in the second dipping procedure is 3 μm). The layer thickness of a γ-alumina supported layer, made without the use of PVA, is typically 8–10 μm after three subsequent dipping procedures with 3 s dipping time. The layer growth for dipping solution, containing PVA is much slower, as stated before, and therefore resulting layer thicknesses after three subsequent dipping procedures under identical conditions are lower. Still layer thicknesses are typically in the order of 5–6 μm after three subsequent dipping procedures.

It is possible to minimize the layer thickness by adapting the dipping parameters in the second and third dipping procedure. For example lowering the concentration of the dipping solution it seems possible to repair the pinholes only. The slipcasting process is then so slow, that the over-all thickness hardly increases. Further optimization can result in only two necessary dipping procedures to obtain γ-alumina films without pinholes.

4.2.2. Structural comparison of non-supported and supported thin films

It was proven, that the structure of non-supported and supported thin γ-alumina films, made without the addition of PVA, resemble each other very closely [7]. In this section it will be shown, that this is also true for films, prepared with the addition of PVA. Non-supported thin films, made with and without PVA, are nearly identical in structure, as was proven before. Therefore, the only unsolved problem is whether the supported thin films, made with and without PVA show similar behaviour. Unless stated otherwise, all thin γ-alumina films in this section are prepared by adding PVA to the boehmite colloidal suspension.

A membrane microstructure is described by three parameters: the (mean) pore diameter and its distribution, the porosity and the tortuosity. Other parameters, like a specific surface area, are directly coupled to these parameters. From N₂ adsorption-desorption data of non-supported thin films, a mean pore diameter (actually the maximum in the pore diameter distribution) and a porosity have been determined before (Table III). The unknown structural parameter is the tortuosity. This parameter was determined by water permeability experiments on supported thin films. To check the values for the three parameters, a cut-off value determination of PEG was performed as well as gas permeability experiments.

In liquid permeation, the volume flux per unit area is proportional to the pressure drop over the membrane, according to Equation 1. From the proportionality constant, a tortuosity can be determined. Fig. 10 gives a representative plot of the volume flux per unit area versus the pressure drop for a supported γ-alumina thin film, calcined at 600 °C. It can be assumed, that the resistance to liquid transport is 99% in the top layer [10]. With this assumption and considering the structural data in Table III, the product of $k_0 k_f$ can be calculated with the bulk viscosity of water at 22.0 °C (see Equation 1). The value found is

TABLE III Mean values of important structural data of thin γ -alumina films, calcined at 600 °C, made with addition of PVA

Pore radius (nm)	Porosity (%)	BET surface ($\text{m}^2 \text{g}^{-1}$)	Tortuosity ($\text{m}^2 \text{g}^{-1}$)
1.5 ^a	51 ^a	250 ^a	5 ± 1 ^b

^a = from non-supported films; ^b = from supported films.

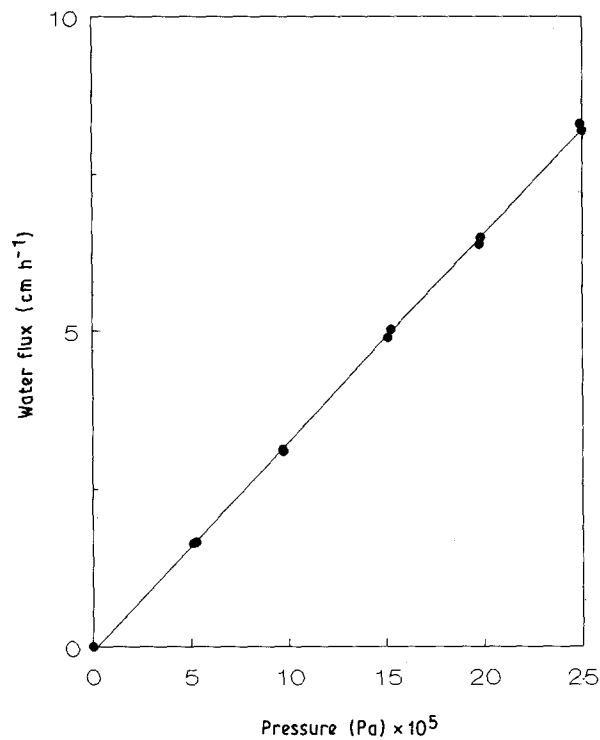


Figure 10 The volume flux per unit area as a function of the pressure drop in a water permeability experiment, performed on a supported thin γ -alumina film (made with PVA) at a temperature of 22.0 °C.

14 ± 3 . The numerical value for k_0 depends on the shape of the pores and is assumed to be 2.6 for slit-shaped pores [19]. With this k_0 a value for the tortuosity, k_t is found to be 5.5 ± 1 .

The Kozeny-Carman constant [10] $K (= k_0 \cdot k_t)$ is normally assumed to be 5. Leenaars however found a value of 13, in good agreement with the above found value of 14. These unusual high tortuosities are attributed to the card pack like structure of the plate-shaped γ -alumina particles. Since the length is much larger than the slit width, the path to be travelled to bridge a certain width, is very long (Fig. 4b). Therefore the tortuosity, which is defined as the square of the ratio of the path to be travelled and the actual width crossed, is very high. It should be noticed, that the values calculated for the tortuosity are very sensitive to slight structural changes like the porosity and the internal surface area. This makes an exact determination of the tortuosity very difficult. Still the fact, that the tortuosity found above and the tortuosity as found by Leenaars are so close, supports the assumption, that the structure of supported γ -alumina films made with and without PVA are closely connected. Consequently the mean pore diameters of the supported γ -alumina thin films can be predicted from the non-supported γ -alumina thin films.

To experimentally estimate the pore diameter of the supported γ -alumina thin films the rejection characteristics of these membranes for PEG were determined. These experiments were also performed by Leenaars [8]. His results (code Al_2O_3 -400 and Al_2O_3 -800) and the results for the newly formed supported films (dipped three times with PVA, code Al_2O_3 -600) are brought together in Fig. 11 and Table IV. The number denotes the calcination temperature. The supported thin film calcined at 400 °C will have the smallest pore diameter and thus the lowest cut-off value. The solute retention (SR) is defined as $\text{SR} = 1 - C_p/C_f$, where C_p and C_f are the solute concentration in the permeate and feed, respectively. The cut-off value, which is the molecular weight of a solute for which a retention value of 90% is reached, appears to be 2000 for Al_2O_3 -400, about 6000 for Al_2O_3 -600 and 20000 for Al_2O_3 -800. From this it can be seen, that the mean pore diameter of the Al_2O_3 -600, made with addition of PVA, falls in between the mean pore diameter of Al_2O_3 -400 and Al_2O_3 -800. This further supports the assumption, that the structure of supported γ -alumina films made with and without PVA are closely connected. From Table IV finally it is clear that membrane fouling did not occur in any case. The product flux hardly declines with the type of PEG dissolved and is nearly equal to the clean water flux during at least 1 h.

Table IV also compares the gyration radius of the PEG molecules with the mean pore diameter of the γ -alumina thin films, as predicted from non-supported films. It can be seen, that the cut off-values are in reasonable agreement with the mean pore diameter of the thin film. It should be remarked, that the solute retention is not only dependent on the pore diameter of the porous medium, but also on the shape of the molecule with respect to that of the pore and the interaction between the solute molecule and the membrane. Some authors [16,20] tried to correct for this influence, thus coupling retention data to the structural data. This is very questionable however. That the interaction between the membrane and the solute can be very strong, was shown in a single filtration experiment. In this experiment, waste water from an off-shore gas platform was filtrated with a supported γ - Al_2O_3 -600 thin film. Table V presents the most important contaminations and their retention values. These are surprisingly high and cannot be accounted for by the ratio of solute and pore radii alone.

From the previous experiments, it was qualitatively established, that the structure of supported thin films, made with and without PVA, is similar. A final quantitative confirmation is given by helium gas permeability experiments. For this purpose, γ -alumina thin films were applied on three different types of support (Table VI). Type 1 supports contains pores of 0.15 μm diameter, type 2 contains pores of 0.4 μm in diameter and type 3 is a multi-layer support. This consisted of a support with a mean pore diameter of 5 μm and a 30 μm thick intermediate layer, containing pores of 0.2 μm diameter. It was not possible to make pinhole free thin films on types 2 and 3 supports without addition of PVA, probably due to the larger pore

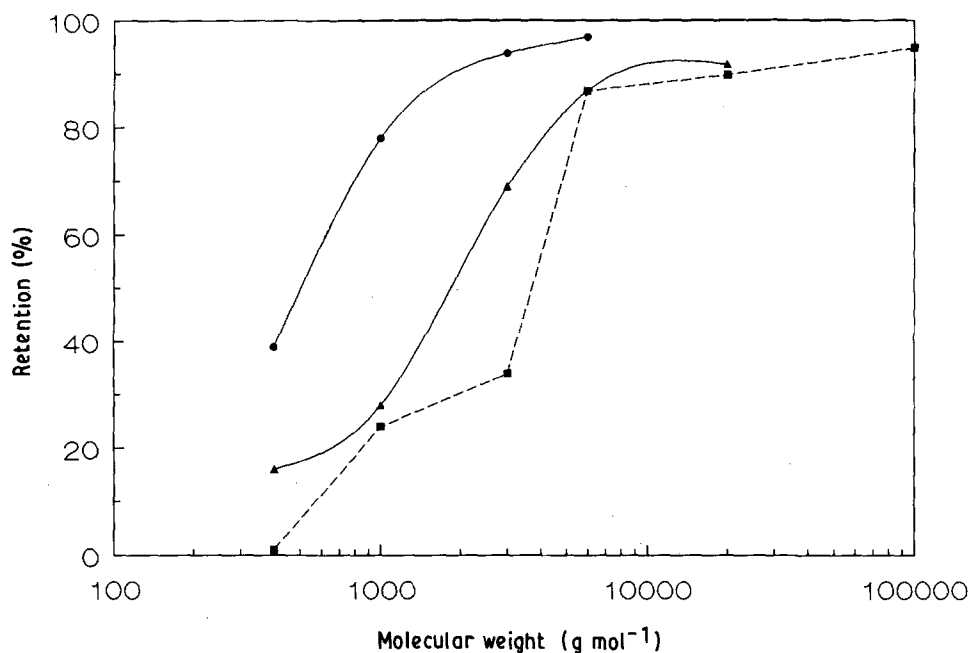


Figure 11 Solute retention as a function of the molecular weight of polyethylene glycol polymers for several supported thin films: (○) Al₂O₃-400 = calcined at 400°C, data Leenaars [8], (▲) Al₂O₃-600 = calcined at 600°C, PVA added, data this paper; (□) Al₂O₃-800 = calcined at 800°C, data Leenaars [8].

TABLE IV Solute retention and flux data for PEG polymers of different molecular weight, filtered by three types of alumina supported thin films: Al₂O₃-400 = calcined at 400°C, data Leenaars [8], Al₂O₃-600 = calcined at 600°C, PVA added, data this paper, Al₂O₃-800 = calcined at 800°C, data Leenaars [8]

Molecular weight PEG	Gyration radius (nm)	Al ₂ O ₃ -400 ^a SR (%)	flux m s ⁻¹ Pa ⁻¹ (× 10 ⁻¹¹)	Al ₂ O ₃ -600 ^b SR (%)	flux m s ⁻¹ Pa ⁻¹ (× 10 ⁻¹¹)	Al ₂ O ₃ -800 ^c SR (%)	flux m s ⁻¹ Pa ⁻¹ (× 10 ⁻¹¹)
Pure water	-	-	0.39	-	0.81	-	3.1
400	0.9	39	0.39	19	0.81	1	3.1
1000	1.3	78	0.39	28	0.78	24	3.1
3000	1.7	94	0.36	69	0.81	34	3.1
6000	2.5	97	0.33	88	0.75	87	3.1
20000	4.0	-	-	92	0.75	90	3.1

^a = mean pore diameter 2.7 nm; ^b = mean pore diameter 3 nm; ^c = mean pore diameter 4.8 nm.

TABLE V Solute retention of the main contaminations in waste water of an off-shore gas platform, filtered over a γ-Al₂O₃-600 supported thin film, made with PVA

Component	Feed concentration (p.p.m.)	Filtrate concentration (p.p.m.)	SR (%)
Benzene	315	25	92
Toluene	125	7	94
Ethylbenzene	7	0.2	97
Xylene	53	3.5	93

diameter or poor wetting of the surface. Therefore on types 2 and 3 supports only gas permeability data of thin films, made with addition of PVA could be obtained. Table VI gives several helium gas permeability data. First the helium permeability for supported γ-alumina thin films, made with and without PVA are presented. These data are corrected for the layer thickness and the supported influence and thus represent normalized values for the top layer only. A difference between these permeabilities must arise from structural differences. Also included are theoretical estimations of the gas permeability, using the structural data of Table III for non-supported thin γ-alumina films

and employing the Knudsen diffusion equation (Table VI).

From Table VI several important features arise. In the first place it can be seen, that gas permeability data on all thin films on type 1 supports are equal. This means there is no structural difference between the thin supported films made with and without PVA. In the second place it can be seen, that the type of support used has no marked influence on the permeability. Therefore the structure of the resulting thin film is independent of the type of support used. Finally Table VI shows that the experimental and theoretical permeability values are in reasonable agreement with

TABLE VI Comparison between experimental and theoretical helium gas permeability at 25 °C (notation F_0^{HE}) for thin supported alumina films, made with and without PVA on several support types; data are corrected for the layer thickness and the support, all films calcined at 600 °C

Support	Formation of layer without PVA	Support resistance (%)	F_0^{HE} no PVA (mol m ⁻¹ m ⁻² s ⁻¹ Pa ⁻¹) (× 10 ¹²)	F_0^{HE} with PVA (mol m ⁻¹ m ⁻² s ⁻¹ Pa ⁻¹) (× 10 ¹²)	F_0^{HE} calculated ^a (mol m ⁻¹ m ⁻² s ⁻¹ Pa ⁻¹) (× 10 ¹²)
Type 1	Yes	65	55 ± 6	57 ± 7	51 ± 7
Type 2	No	40	–	57 ± 3	51 ± 7
Type 3	No	< 10	–	57 ± 2	51 ± 7

^a = calculated by $F_0 = 1.06\epsilon r / (k_s \cdot [\text{RTM}]^{1/2})$ and data of Table III.

each other. Because the theoretical values for the gas permeability were calculated, employing structural data of non-supported thin films, it is directly proven that the structure of non-supported and supported thin films are identical with respect to their effect on gas transport properties. Therefore the structure of non-supported γ -alumina thin films can be used to predict transport properties of supported γ -alumina thin films. It should also be noted that the data on type 3 supports are equal to the data on types 1 and 2 supports. If a type 3 support is used, the resistance of the support to gas phase flow is negligible (< 10%). Therefore the permeability of the thin supported film can be determined directly. The permeabilities of types 1 and 2 supports are calculated from the permeabilities from the support and the support and thin film. Since the data are similar to each other, the calculation procedure employed is proven to be correct. The procedure is fully described elsewhere [13].

5. Conclusions

1. Addition of polyvinylalcohol (0.25 g PVA/g Al₂O₃, molecular weight PVA 72000) to the colloidal boehmite suspension results in higher allowable drying and calcination rates of supported boehmite precursor films. The layer quality of the resulting γ -alumina films is more reproducible. Thus the addition of PVA is necessary to slipcast defect free γ -alumina thin films on supports with a pore diameter of 0.4 μm or smaller or on a multi-layer supports.

2. Addition of PVA to the boehmite colloidal suspension only slightly influences the microstructure of the resulting non-supported or supported thin films.

3. The forming mechanism of supported thin films can also be described by the slipcasting mechanism, when PVA is added to the boehmite colloidal suspension. The layer growth rate is slower however, resulting in thinner supported films under identical circumstances as compared to slipcasting without PVA addition.

4. Pinhole free supported thin γ -Al₂O₃ films are defined by their gas transport characteristics. They can be produced reproducibly only by a multiple dipping technique, using PVA additions. The resulting layer thickness is approximately 5–6 μm after three subsequent dipping procedures, depending on the support type.

5. Transport properties of supported thin films can be predicted from structural data, gathered on non-supported thin films.

Acknowledgement

This research has been possible by financial assistance from the Innovative Research Program Committee.

References

1. A. J. BURGGRAAF and K. KEIZER, in "Inorganic membranes" Ch. II, edited by R. Bhawe (Van Nostrand, New York, 1991).
2. R. SCHNABEL and W. VAULONT, *Desalination* **21** (1978) 249.
3. J. GILLOT, *EPA 0092840 B1* (1987).
4. M. J. GIESELMAN, M. A. ANDERSON, M. D. MOOSE-MILLER and C. G. HILL, *Sep. Sc. Techn.* **23** (1988) 1695.
5. L. COT, C. GUIZARD and A. LARBOT, *Indus. Ceram.* **8** (1988) 143.
6. M. ASAEDA and L. D. DU, *J. Chem. Engng Jpn* **19** (1986) 72.
7. A. F. M. LEENAARS and A. J. BURGGRAAF, *J. Coll. Interf. Sci.* **105** (1985) 27.
8. *Idem.*, *J. Membr. Sci.* **24** (1985) 261.
9. A. F. M. LEENAARS, K. KEIZER and A. J. BURGGRAAF, *J. Mater. Sci.* **19** (1984) 1077.
10. A. F. M. LEENAARS and A. J. BURGGRAAF, *J. Membr. Sci.* **24** (1985) 245.
11. Y. S. LIN, K. J. de VRIES and A. J. BURGGRAAF, *J. Mater. Sci.* **26** (1991) 715.
12. K. P. KUMAR, J. H. L. VONCKEN, C. LIJZENGA, K. KEIZER and A. J. BURGGRAAF, in Proceedings of ICOM '90, Chicago, accepted for publication.
13. R. J. R. UHLHORN, PhD Thesis, University of Twente, Twente, 1990.
14. K. S. W. SING, *Pure & Appl. Chem.* **57** (1985) 603.
15. S. J. GREGG and K. S. W. SING, "Adsorption, surface area and porosity" (Academic Press, London-New York, 1982) Ch. 3.
16. L. ZEMAN and M. WALES, *Sep. Sci. Technol.* **16** (1981) 275.
17. C. A. FINCH, in "Polyvinyl alcohol: properties and applications" edited by C. A. Finch (J. Wiley & Sons, New York, 1973) 183.
18. V. T. ZASPALIS, PhD Thesis, University of Twente, Twente, 1990, Ch. 2 accepted for publication in *J. Mater. Science* (1991).
19. P. C. CARMAN, *Trans. Inst. Chem. Engng* **15** (1937) 150.
20. M. N. SARBOLOUKI, *Sep. Sci. Technol.* **17** (1982) 381.

Received 1 October 1990
and accepted 18 March 1991